# Kinesin-5 regulates the growth of the axon by acting as a brake on its microtubule array

Kenneth A. Myers and Peter W. Baas

Department of Neurobiology and Anatomy, Drexel University College of Medicine, Philadelphia, PA 19104

Kinesin-5 is a homotetrameric motor protein that interacts with adjacent microtubules in the mitotic spindle. Kinesin-5 is also highly expressed in developing postmitotic neurons. Axons of cultured neurons experimentally depleted of kinesin-5 grow up to five times longer than controls and display more branches. The faster growth rates are accompanied by a doubling of the frequency of transport of short microtubules, suggesting a major role for kinesin-5 in the balance of motor-driven forces on the axonal microtubule array. Live-cell imaging reveals that the effects on axonal length of kinesin-5 depletion are caused partly by a lower propensity of the axon and newly forming branches to undergo bouts of retraction. Overexpression of wild-type kinesin-5, but not a rigor mutant of kinesin-5, has the inverse effect on axonal length. These results indicate that kinesin-5 imposes restrictions on the growth of the axon and does so at least in part by generating forces on the axonal microtubule array.

## Introduction

The growth and maintenance of the axon is dependent on a continuous array of microtubules that extends from the cell body of the neuron into the growth cone. Individual microtubules assume a variety of lengths within the array, ranging from <1 to >100 μm (Yu and Baas, 1994). Very short microtubules are able to move rapidly and in both directions (Wang and Brown, 2002). In contrast, the longer microtubules in the axon are essentially immobile (Ma et al., 2004; Ahmad et al., 2006). Twice as many short microtubules move in the anterograde direction, presumably to ensure that more tubulin enters the axon than is moved back to the cell body. In addition to supplying tubulin for axonal growth, mobility within the microtubule array promotes the morphological plasticity underlying events such as growth-cone motility and branch formation (Yu and Baas, 1994; Dent et al., 1999). The longer microtubules are important too because they act as compression-bearing struts that prevent the axon from retracting under the myosin-II–based contractile forces imposed on the cortical actin (Myers et al., 2006b). We have proposed a model whereby the same molecular motors that transport the short microtubules impinge upon the long microtubules to regulate the degree to which they can resist the myosin-based contractile forces (Baas et al., 2006).

We have begun to study the panoply of microtubule-based motors that generate forces against long and short microtubules. We have found that if we deplete cytoplasmic dynein or if we depolymerize actin filaments, the frequency of anterograde microtubule transport is reduced by about half (Hasaka et al., 2004; He et al., 2005). These results are consistent with a scenario in which short microtubules move anterogradely via a "sliding filament" mechanism in which the cargo domain of the motor interacts (indirectly) with actin filaments (Pfister, 1999; Myers et al., 2006a). The motor domain is then available to transport the short microtubules. Consistent with our model for long and short microtubules, depletion of cytoplasmic dynein also renders the long microtubules less capable of resisting the myosin-II–based contractile forces that cause the axon to retract (Ahmad et al., 2000; Myers et al., 2006a). The fact that not all of the mobility within the microtubule array depends on cytoplasmic dynein indicates that there are other participating motors, presumably kinesins.

The relevant kinesins are the so-called mitotic kinesins, which generate forces between adjacent microtubules rather than between microtubules and membranous cargo (Dent et al., 1999). We have shown that many of these specialized kinesins continue to be expressed in terminally postmitotic neurons (Sharp et al., 1997; Ferhat et al., 1998; Buster et al., 2003). We are particularly interested in kinesin-5 (also known as Eg5), which forms homotetramers consisting of two sets of antiparallel motor domains (Kashina et al., 1996). In the mitotic spindle, the primary function of kinesin-5 is to maintain spindle bipolarity by generating centrosome-directed forces between antiparallel microtubules in the midzone (Blangy et al., 1995; Sharp et al., 1999a,b; Kapitein et al., 2005). In neurons, pharmacological inhibition of kinesin-5

Correspondence to Peter W. Baas: pbaas@drexelmed.edu

Abbreviations used in this paper: DIC, differential interference contrast; PDL, poly-D-lysine.

The online version of this article contains supplemental material.


The Journal of Cell Biology, Vol. 178, No. 6, September 10, 2007 1081–1091
http://www.jcb.org/cgi/doi/10.1083/jcb.200702074

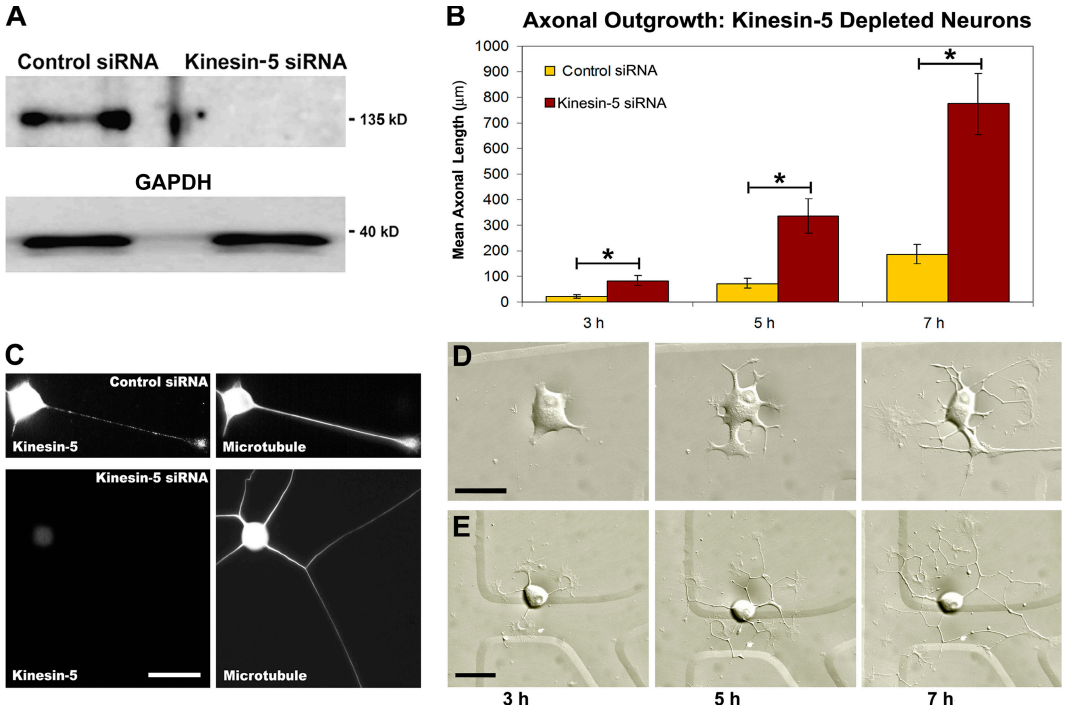


Figure 1. **Kinesin-5 depletion results in increased axonal length.** (A) Western blot showing kinesin-5 protein levels in cultured sympathetic neurons treated with control siRNA and kinesin-5 siRNA. The bottom panel shows the glyceraldehyde-3-phosphate dehydrogenase (GAPDH) loading control for both protein samples. (B) Quantification of mean axonal outgrowth reveals significantly longer axons of kinesin-5–depleted neurons at all time points observed, with a 4.3-fold mean increase in axonal length (mean ± SEM; 3 h, control = 21.3 ± 6.45 μm, experimental = 82.8 ± 19.7 μm; 5 h, control = 71.8 ± 20.0 μm, experimental = 335 ± 66.8 μm; 7 h, control = 187 ± 37.1 μm, experimental = 774 ± 120 μm) (control siRNA, $n = 17$; kinesin-5 siRNA, $n = 21$; *, $P < 0.01$). (C) Fluorescence images of kinesin-5 immunostaining in control siRNA (top) and kinesin-5 siRNA–treated neurons (bottom). The corresponding microtubule staining for these two cells is shown in the panels on the right. (D) DIC images of a control siRNA neuron taken at 3, 5, and 7 h after replating. (E) DIC images of a kinesin-5–depleted neuron at 3, 5, and 7 h after replating revealed the notable increases in axonal length quantified in B. Bars, 20 μm.

results in longer axons (Haque et al., 2004; Yoon et al., 2005), suggesting a key role for this motor in the development of the nervous system. In the present study, we have investigated the underlying mechanisms by which kinesin-5 influences the development of the axon.

## Results

Although monastrol (the drug used in the earlier studies on neurons; Haque et al., 2004; Yoon et al., 2005) is quite specific for kinesin-5 (Kapoor et al., 2000; Maliga et al., 2002; Kwok et al., 2006; Maliga and Mitchison, 2006), we wished to pursue an additional approach that would deplete kinesin-5 rather than inhibit it. For this we used siRNA, which has been shown to be highly effective at depleting kinesin-5 from other cell types (Weil et al., 2002). For the current experiments, rat sympathetic neurons were transfected with 10 μM siRNA (control or kinesin-5), plated densely on plastic dishes, and then allowed time for the protein to be depleted. As determined by Western blotting, 3 d after transfection was sufficient time to deplete over 95% of the kinesin-5 protein from the neurons (Fig. 1 A). The neurons were then replated at a lower density onto glass coverslips treated with polylysine and laminin, and allowed to grow axons anew. For some studies, we also performed side-by-side monastrol experiments.

### Effects of kinesin-5 depletion on axonal morphology

For evaluation of the effects of siRNA-based depletion of kinesin-5 on axonal morphology, neurons were chosen randomly and then imaged at successive time points beginning 1 h after plating, and continuing every 2 h thereafter until 7 h. Although at the 1 h time point there were very few neurons that had extended axons in either the control or experimental groups; analyses of mean axonal length at 3, 5, and 7 h all revealed significant increases in the experimental neurons. Specifically, quantification of axonal length revealed a 4.3-fold increase in mean axonal lengths at all three time points, a change that was statistically significant (3 h, $P < 0.008$; 5 h, $P < 0.002$; 7 h, $P < 0.0003$; two-tailed $t$ test; Fig. 1 B). These differences (Fig. 1, C and D) were comparable to those obtained in parallel experiments using monastrol (see Fig. 8).

In addition to being longer, the experimental axons were also more branched than the control axons (Fig. 2, A and B). For quantification of this effect, total branch numbers were normalized to total axonal length, so that the values were comparable between control and kinesin-5–depleted neurons (control, $n = 27$; kinesin-5 siRNA, $n = 37$). Statistical analyses of axonal branching data revealed a significant increase in branching frequency of kinesin-5–depleted neurons to levels nearly four times higher than controls (Fig. 2 C). When branching frequency was quantified based on the location of the branches, a statistically

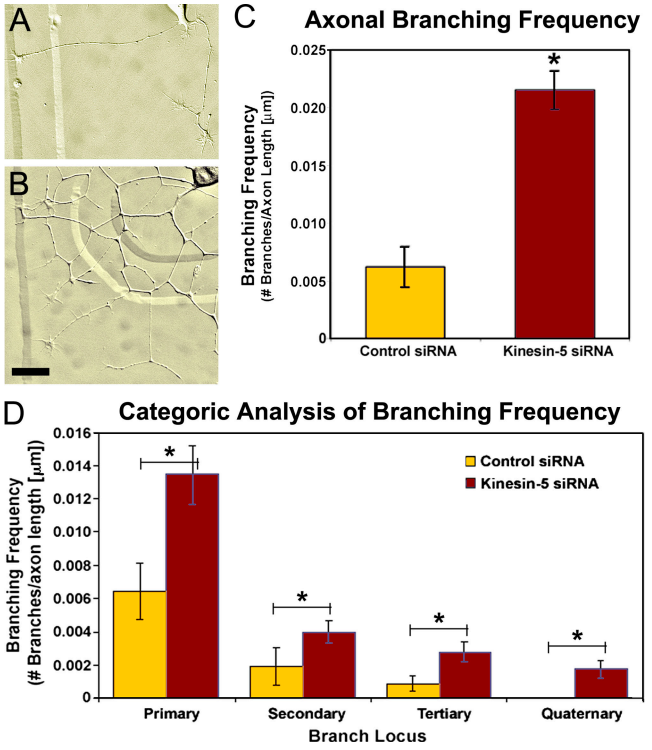


Figure 2. **Axonal branching is enhanced when kinesin-5 is depleted.** (A and B) DIC images of typical control (A) and kinesin-5–depleted (B) neurons. Note the increase in branch number in axons depleted of kinesin-5. (C) Quantitative analysis of axonal branch number (normalized to total axonal length) revealed a statistically significant increase when compared with control siRNA–treated neurons (mean ± SEM; control siRNA = 0.006 ± 0.002, kinesin-5 siRNA = 0.022 ± 0.002; *, $P = 5.76 \times 10^{-8}$). (D) Categorical analysis at various branching loci (control siRNA, $n = 27$; kinesin-5 siRNA, $n = 37$) revealed a statistically significant increase in branching frequency at all branch positions (mean ± SEM; primary branch: control = 0.006 ± 0.002, kinesin-5 siRNA = 0.013 ± 0.002, *, $P < 0.02$; secondary branch: control = 0.002 ± 0.001, kinesin-5 siRNA = 0.004 ± 0.001, *, $P < 0.03$; tertiary branch: control = 0.001 ± 0.0004, kinesin-5 siRNA = 0.003 ± 0.001, *, $P < 0.03$; quaternary branch: control = 0.00 ± 0.00, kinesin-5 siRNA = 0.001 ± 0.0005, *, $P < 0.007$). Bars, 20 μm.

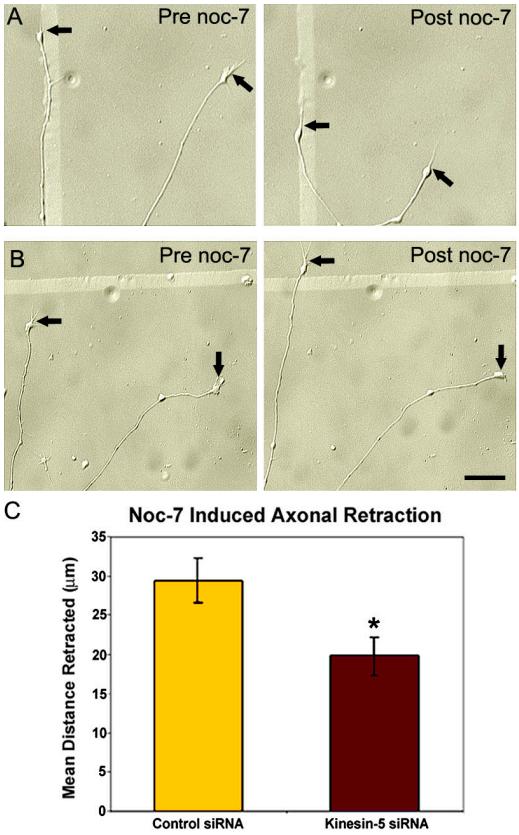


Figure 3. **Depletion of kinesin-5 reduces the distance of axonal retraction.** (A and B) DIC images of control axons (A) and kinesin-5–depleted axons (B) before and 30 min after treatment with 0.3 mM noc-7. (B) Kinesin-5–depleted axons continue to elongate even in the presence of noc-7. Arrows demarcate the distal tips of growth cones before and after noc-7 treatment. (C) Quantitative analysis of noc-7–induced axonal retraction revealed a statistically significant reduction in mean distance retracted in neurons depleted of kinesin-5 (mean ± SEM; control, $n = 54$; kinesin-5 siRNA, $n = 55$; *, $P = 0.011$). Bar, 20 μm.

significant increase in branching frequency was identified in kinesin-5–depleted neurons at all branch loci (Fig. 2 D). In neurons depleted of kinesin-5, primary branch frequency was increased to 217% of controls ($P < 0.02$; $n = 14$), secondary branch frequency was increased to 200% of controls ($P < 0.03$; $n = 14$), and tertiary branch frequency was elevated to 298% of control neurons ($P < 0.03$; $n = 12$). There were no quaternary branches observed in the control siRNA group of neurons during the observation time period ($n = 12$). The change between control and kinesin-5 siRNA was found to be statistically significant ($P < 0.007$).

We next investigated whether the kinesin-5–depleted axons differed from controls in their propensity to retract in response to physiological cues. For this, we used noc-7 (a donor of nitric oxide and potent inducer of axonal retraction; Ernst et al., 2000; He et al., 2002). After allowing neurons depleted of kinesin-5 to undergo 12–16 h of axonal growth, differential interference contrast (DIC) images were taken of individual neurons whose axons were >100 μm, followed by treatment with 0.3 mM noc-7 for 30 min. These same neurons were then relocated and imaged once again, and the before-and-after images were analyzed for mean differences in axonal length. Quantification of mean distance retracted revealed that the axons of neurons transfected with control siRNA underwent significantly greater distances of retraction than the axons of neurons depleted of kinesin-5 (control siRNA, $n = 54$; kinesin-5 siRNA, $n = 55$). In some cases, the axons of the neurons depleted of kinesin-5 actually continued to grow in the presence of noc-7, which virtually never occurred in the case of the controls (Fig. 3, A and B). On average, neurons treated with control siRNA retracted their axons 29.5 ± 2.87 μm after 30-min exposure to noc-7, whereas neurons depleted of kinesin-5 retracted their axons 19.8 ± 2.45 μm (mean ± SEM, $P = 0.011$; Fig. 3 C). Thus depletion of kinesin-5 reduces the distances over which the axons would normally have retracted. Similar results were obtained with monastrol (unpublished data).

### Effects of kinesin-5 depletion on axonal transport of short microtubules

For studies on microtubule transport (Fig. 4 A), the culture regimes were the same as for the morphological studies, except that replating was performed at 60 h after transfection, and cells

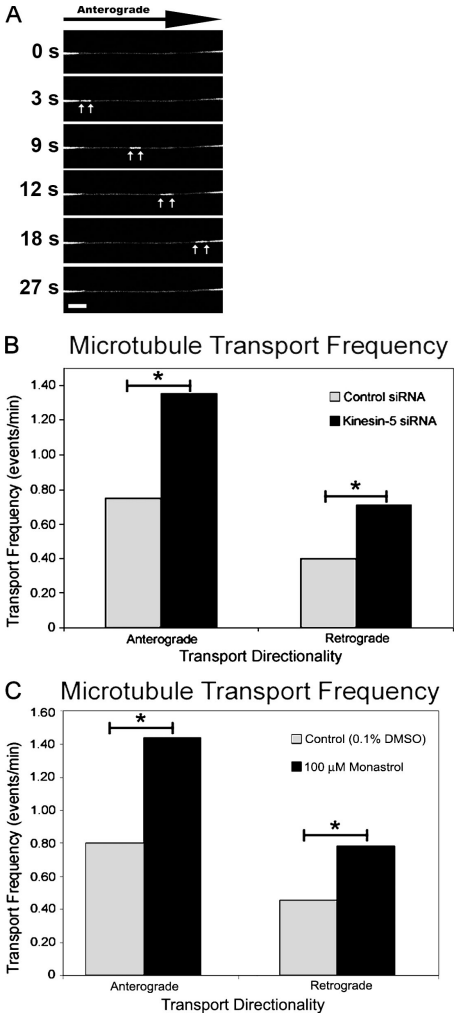


Figure 4. **Depletion of kinesin-5 enhances the transport frequency of short microtubules.** (A) Time-lapse images of a neuron expressing GFP-tubulin reveal a short microtubule moving in the anterograde direction through a photobleached axon. White arrows mark the leading and trailing ends of the microtubule. (B) Quantification of short microtubule transport frequency using siRNA-based depletion of kinesin-5 resulted in the increased frequency of bidirectional short microtubule transport (anterograde: control siRNA, 0.752 events/min; kinesin-5 siRNA, 1.35 events/min; retrograde: control siRNA, 0.400 events/min; kinesin-5 siRNA, 0.705 events/min; *, $P \leq 0.025$). (C) Inhibition of kinesin-5 with monastrol produced a result similar to siRNA-based depletion of kinesin-5, with an increase in bidirectional transport frequency to levels approximately twofold higher than observed in control neurons (anterograde: DMSO, 0.801 events/min; monastrol, 1.438 events/min; retrograde: DMSO, 0.458 events/min; monastrol, 0.788 events/min; *, $P < 0.01$). Bar, 5 μm.

were allowed to grow axons for 12–16 h before imaging. These times were used because they coincide with the depletion of kinesin-5 via siRNA (Fig. 1 A) and because this period of incubation is optimal for EGFP-tubulin expression in these cells. For control siRNA, the total number of movements was 121 over a period of 105 min of image acquisition, with 79 in the anterograde direction and 42 in the retrograde direction. For kinesin-5 siRNA, the total number of movements over 105 min of imaging was 216, representing the sum of 142 movements in the anterograde direction and 74 movements in the retrograde direction. With respect to transport directionality, these data represent a 179% increase over controls in anterograde movement frequency, and a 176% increase over controls in retrograde movement frequency, both statistically significant increases (anterograde, $P \leq 0.01$; retrograde, $P \leq 0.025$; $\chi^2$; Fig. 4 B). Enhanced frequencies of short microtubule transport were also observed when monastrol was used to inhibit kinesin-5 activity, and these changes were comparable to the siRNA experiments (Fig. 4 C). For the monastrol studies, there was a 178% increase in anterograde transport frequency and a 172% increase in retrograde transport frequency (anterograde, $P < 0.001$; retrograde, $P < 0.001$; $\chi^2$). These results suggest that kinesin-5 imposes limitations on the number of short microtubules that are in transit (in both directions) within the axon.

To investigate whether this effect on transport is specific to microtubules, we added fluorescently labeled markers of either vesicles or mitochondria and analyzed their movements under control- and kinesin-5–inhibited conditions. Using a rhodamine–dextran tracer to monitor pinocytosed vesicular transport (Fig. 5 A), we found that there was no statistical variation in axonal vesicle trafficking under conditions of kinesin-5 depletion in either the distance or direction that the moving vesicles were transported (anterograde, $P = 0.232$; retrograde, $P = 0.431$; two-tailed *t* test; Fig. 5 B). We next investigated the effects of kinesin-5 depletion on the axonal transport of mitochondria using the mitotracker label, which is a fluorescent label that is specific for mitochondria (Buckman et al., 2001). For these experiments we measured both the length of the mitochondria, as well as the distance moved during the imaging period. Stationary mitochondria were not analyzed, although there was no noticeable difference between the numbers of stationary mitochondria between control and kinesin-5–depleted neurons (unpublished data). Similar to our studies of vesicle transport, no statistical difference was found when mitochondrion lengths were compared between control and kinesin-5–depleted axons ($P = 0.08$, two-tailed *t* test). Analysis of mitochondrion transport distances revealed a similar, nonsignificant variation between control and kinesin-5–depleted specimens ($P = 0.677$, two-tailed *t* test; Fig. 5, C and D). These data are consistent with the effects of kinesin-5 on axonal transport being specific to the transport of microtubules.

### Depletion of kinesin-5 accelerates axonal growth by decreasing stepwise retraction events

Live-cell movies were used to further investigate the effects of depleting kinesin-5 on axonal length. Phase-contrast images were acquired for 5 h at 3-min intervals beginning 2 h after the neurons were replated. Consistent with the still images (Figs. 1 and 2), the movies show that axons depleted of kinesin-5 grow more rapidly and undergo dramatic increases in branching as compared with controls (Fig. 6 A). The movies indicate that these effects are due, at least in part, to diminution in retraction events that normally accompany axonal development. Control neurons undergo relatively consistent bouts of growth and retraction, with the net result being axonal elongation. In contrast, kinesin-5–depleted neurons undergo substantially fewer bouts of retraction, resulting in enhanced stepwise growth. Analysis of the data indicates a significant change in the distribution of

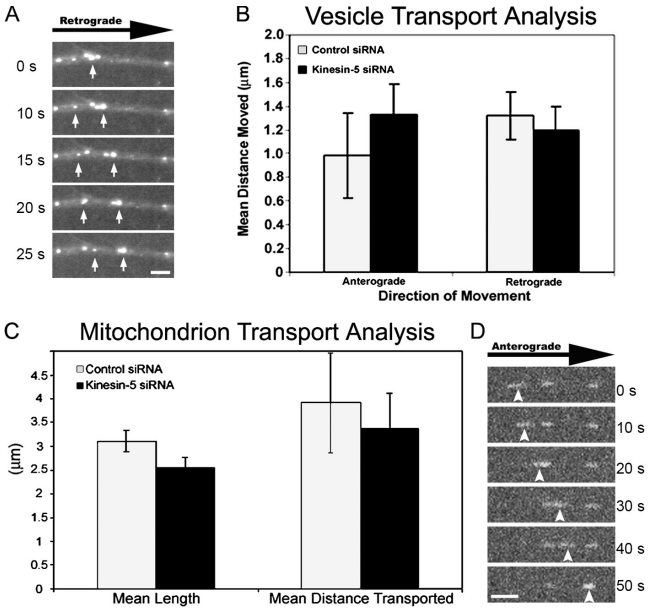


Figure 5. **Depletion of kinesin-5 motor does not affect axonal transport of membranous elements.** (A) Time-lapse images of rhodamine-dextran–labeled vesicles being transported retrogradely within the axon. White arrows demarcate two mobile vesicles observed during the period of imaging. (B) Quantification of vesicular transport direction and frequency revealed no difference between control and kinesin-5–depleted neurons (mean ± SEM; anterograde: control = 0.983 ± 0.357, kinesin-5 = 1.33 ± 0.262; retrograde: control = 1.32 ± 0.201, kinesin-5 = 1.19 ± 0.206) (control axons, $n = 14$; kinesin-5–depleted axons, $n = 14$). (C) Analysis of mitochondrion transport revealed that the depletion of kinesin-5 does not have an effect on mitochondrion length (mean length ± SEM; control = 3.10 ± 0.232 μm, kinesin-5 siRNA = 2.55 ± 0.206 μm) or distance of transport (mean ± SEM; control = 3.91 ± 1.05 μm, kinesin-5 siRNA = 3.37 ± 0.742 μm) (control siRNA, $n = 38$; kinesin-5 siRNA, $n = 39$). (D) Time-lapse images of a mitotracker FM–labeled mitochondrion being transported anterogradely within the axon. Arrowheads mark the moving mitochondrion. Bars, 5 μm.

growth steps and retraction steps between control neurons and neurons depleted of kinesin-5 (control, $n = 13$; kinesin-5 siRNA, $n = 13$; $P \leq 0.001$; $\chi^2$) (Fig. 6, B and D). The effect on retraction was even more dramatic with regard to the stepwise movements of axonal branches, commonly resulting in branches that retracted entirely back into the primary axon (control, $n = 8$; kinesin-5 siRNA, $n = 13$; $P \leq 0.001$; $\chi^2$; Fig. 6 C and Video 1, available at http://www.jcb.org/cgi/content/full/jcb.200702074/DC1). Of the 198 stepwise movements measured in control branches, 112 were growth oriented, whereas 68 were retractile, and the remaining 18 constituted time points when the axon did not grow or retract (neutral steps). In neuronal branches that had been depleted of kinesin-5, a total of 356 stepwise movements were recorded, the sum of 298 growth-oriented, 34 retractile, and 24 neutral steps (Fig. 6 E). Thus, it appears that depletion of kinesin-5 results in enhanced frequencies of axonal branching by causing the axon to retract branches less frequently, thus allowing greater numbers of branches to persist.

### The effects of kinesin-5 overexpression are the inverse of kinesin-5 depletion

We wished to further test the specificity of our results by ascertaining whether an increase in kinesin-5 produces the inverse effect of depletion. To investigate this, neurons were transfected to express either GFP alone (control) or to express EGFP–kinesin-5, after which they were replated and allowed to grow axons for 7 h, as described for the siRNA experiments. For these experiments, we used mCherry-tubulin to visualize microtubule transport. Investigations of mean axonal length in GFP control neurons ($n = 20$) were analyzed at 3, 5, and 7 h after replating. Axons were found to be of similar lengths to controls from siRNA-based experiments from respective time points (mean ± SEM; GFP control, 3 h = 64.5 ± 10.2 μm, 5 h = 108 ± 16.1 μm, 7 h = 205 ± 21.3 μm). Consistent with the prediction of adding a large number of additional kinesin-5 molecules, the most highly expressing neurons displayed very short axons (typically <30 μm; Fig. 7 B). Comparison of axonal lengths of the low expressers ($n = 21$; Fig. 7 A) revealed a statistically significant decrease in mean axonal length when compared with GFP controls at all three observed time points (3 h, $P < 0.004$; 5 h, $P < 0.004$; 7 h, $P < 0.0005$; two-tailed $t$ test; Fig. 7 C). When normalized to controls, these reductions represent a decrease of 252, 225, and 209% (at 3, 5, and 7 h, respectively) in the mean axonal lengths of neurons expressing EGFP–kinesin-5.

We next analyzed microtubule transport in the axons of the low expressers (Fig. 7 A). Analysis of GFP control neurons revealed frequencies of short microtubule transport that did not differ significantly from control siRNA–treated transport frequencies. For GFP control axons, the total number of movements was 93, with 60 in the anterograde direction and 33 in the retrograde direction over a period of 77 min of image acquisition. For EGFP–kinesin-5–expressing neurons, the total number of movements was 82, with 40 in the anterograde direction and 42 in the retrograde direction over 98 min of image acquisition. The decrease in transport was statistically significant, but only in the anterograde direction, where EGFP–kinesin-5 expression reduced transport by 190% (anterograde, $P \leq 0.01$; retrograde, $P \leq 1$; $\chi^2$; Fig. 7 D). These results further demonstrate the capacity of kinesin-5 to restrict the number of microtubules in transit, but suggest that kinesin-5 may have a preference for restricting transport in the anterograde direction. There were no notable effects on microtubule bundling or organelle distribution associated with the overexpression of kinesin-5 at these levels (unpublished data).

### Kinesin-5 elicits its effects in a force-dependent manner

It is noteworthy that monastrol-based inhibition of kinesin-5 produced indistinguishable results from siRNA-based depletion of kinesin-5 in all of our studies on axonal morphology (Fig. 8) and microtubule transport (Fig. 4). Monastrol functions as an allosteric inhibitor of the motor by preventing the release of ADP bound to kinesin-5 (Lockhart and Cross, 1996). The functional outcome of this allosteric inhibition is the locking of the kinesin-5 motor in a weak and diffusible microtubule-binding state, capable of eliciting a reduced and passive drag against microtubules in motility assays (Crevel et al., 2004). Thus, treatment with monastrol would eliminate the force-generating properties of kinesin-5 but would presumably not eliminate other properties of kinesin-5, such as its capacity to passively interact with

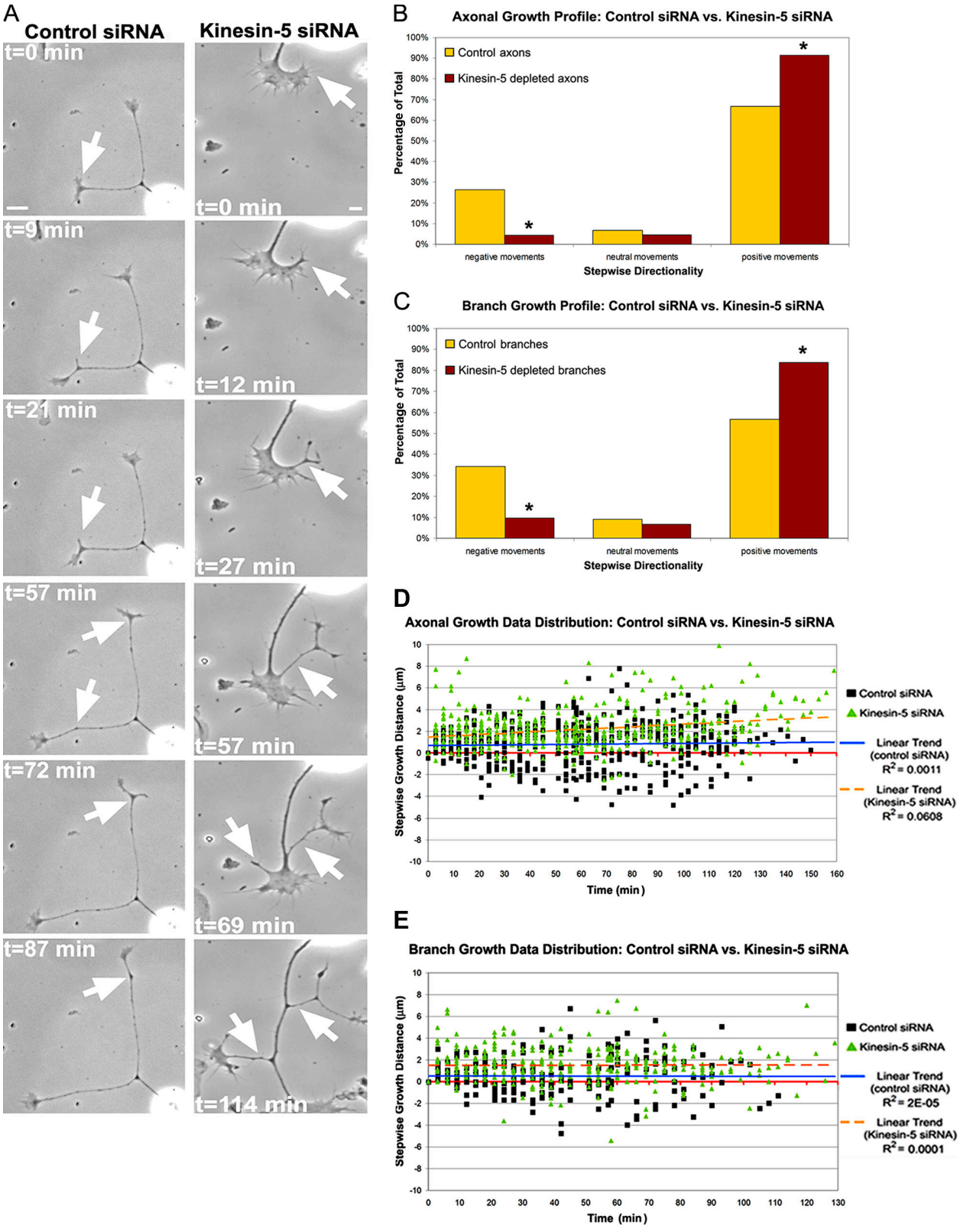


Figure 6. **Kinesin-5 depletion results in fewer bouts of retraction of axons and axonal branches.** (A) Time-lapse, phase-contrast images of a control (left) and a kinesin-5–depleted neuron (right). Notice that whereas control axons form early branches, the branches typically undergo retraction events (left, arrows). Kinesin-5–depleted branches display robust growth and are typically observed to elongate (right, arrows). (B) Quantitative comparison of axonal growth profiles revealed a significant shift toward stepwise bouts of growth in axons depleted of kinesin-5 (*, $P \leq 0.001$; $\chi^2$). (C) Analysis of branching profiles revealed a similar and significant shift toward stepwise bouts of growth when kinesin-5 was depleted (*, $P \leq 0.001$; $\chi^2$). (D and E) Data distribution graphs of the stepwise growth/retraction of control and kinesin-5–depleted axons (D) and branches (E). Bars, 20 μm.

neighboring microtubules and potentially displace other motors, preventing them from interacting with the microtubules. Therefore, it would appear that kinesin-5 must elicit forces in order for it to exert its regulatory effects on axonal growth. To further test this, we expressed in cultured neurons either a wild-type EGFP–kinesin-5 construct or an EGFP-labeled ATPase rigor mutant of kinesin-5 (T112N point mutant). Originally studied by Blangy et al. (1998), this mutation blocks ATP hydrolysis, locking the kinesin-5 motor in a strong microtubule-binding state that is able to promote microtubule–microtubule interactions, but is unable to generate forces against microtubules. In conducting these experiments, we decided to perform them on neurons that had been treated with either control or kinesin-5 siRNA. This experimental approach allowed us to test whether the observed effects on axonal growth require the force-generating properties of the motor and also provided an opportunity to conduct an additional control regarding the specificity of the results observed with siRNA-based depletion of kinesin-5. EGFP fluorescence intensity was used to ensure that we compared similarly expressing cells in each experimental group. There was some initial concern that the kinesin-5 siRNA that persisted in the cells might impede our capacity to express the EGFP–kinesin-5 at sufficiently high concentrations to elicit an effect, but this did not prove to be a problem. The results of these experiments are shown in Fig. 8.

Expression of the wild-type kinesin-5 in neurons treated with control siRNA confirmed our earlier overexpression data (Fig. 7 C), resulting in axonal lengths that were significantly shorter than neurons expressing endogenous levels of kinesin-5 (control siRNA alone, mean ± SEM = 187 ± 37.1 μm; control siRNA + wild-type kinesin-5, 121 ± 29.9 μm; $P < 0.008$, two-tailed *t* test). This effect was not observed in control siRNA–treated neurons expressing the rigor mutant. Rather, under these conditions, expression of the rigor mutant kinesin-5 produced mean axonal lengths nearly identical to control cells (control siRNA + rigor mutant, mean ± SEM = 171 ± 58.2 μm; control siRNA alone, 187 ± 37.1 μm; $P = 0.471$, two-tailed *t* test).

Rescue of kinesin-5–depleted neurons with the wild-type construct resulted in axonal lengths that were statistically similar to neurons treated with control siRNA alone after 7 h of growth (wild-type rescue, mean ± SEM = 257 ± 46.1 μm; control siRNA alone, 187 ± 37.1 μm; $P > 0.05$, two-tailed *t* test). When the rigor mutant was introduced into kinesin-5– depleted neurons, mean axonal lengths were observed to be statistically indistinguishable from those recorded in neurons treated with monastrol or kinesin-5 siRNA alone (rigor mutant rescue, mean ± SEM = 546 ± 86.5 μm, $n = 17$; monastrol, 722 ± 97.9 μm, $n = 17$; kinesin-5 siRNA alone, 774 ± 120 μm, $n = 21$; $P = 0.135$, two-tailed *t* test). Moreover, when compared with other experimental treatments, axonal lengths in the rigor mutant rescue group persisted at levels twice as long as the wild-type rescue group, and nearly three times longer than neurons treated with control siRNA alone (wild-type rescue, 257 ± 46.1 μm, $P < 0.02$; control siRNA alone, 187 ± 37.1 μm, $P < 0.001$, two-tailed *t* test; Fig. 8). These data indicate that the force-generating properties of kinesin-5 are central to its capacity to restrict axonal lengths.

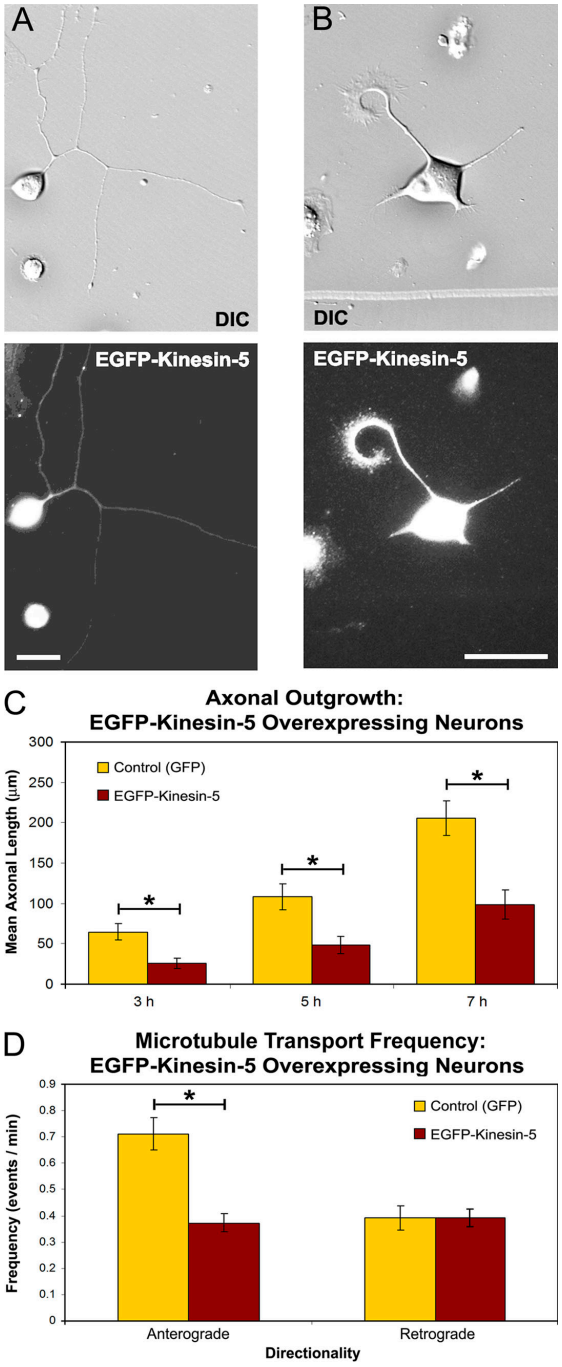


Figure 7. **Axonal growth and microtubule transport frequency are affected by kinesin-5 overexpression.** (A and B) DIC (top) and corresponding anti-GFP immunocytochemistry (bottom) in neurons transfected with a wild-type EGFP–kinesin-5 construct demonstrating that axon length is coordinated with the level of EGFP–kinesin-5 expression. (C) Quantitative analysis of mean axonal length revealed a statistically significant reduction in mean axonal length in neurons expressing EGFP–kinesin-5 when compared with GFP control axons (mean ± SEM; EGFP–kinesin-5: 3 h = 25.6 ± 6.38 μm, 5 h = 48.1 ± 10.7 μm, 7 h = 98.1 ± 18.2 μm; *, $P < 0.0005$). (D) Analysis of short microtubule transport frequency in EGFP–kinesin-5 expressers revealed a significant reduction in anterograde transport, but no change in retrograde transport frequency (mean ± SEM; anterograde: GFP control = 0.779 ± 0.041 events/min; EGFP–kinesin-5 = 0.408 ± 0.016 events/min; retrograde: GFP control = 0.429 ± 0.033 events/min; EGFP–kinesin-5 = 0.449 ± 0.017 events/min; *, $P \leq 0.01$). Bars, 30 μm.

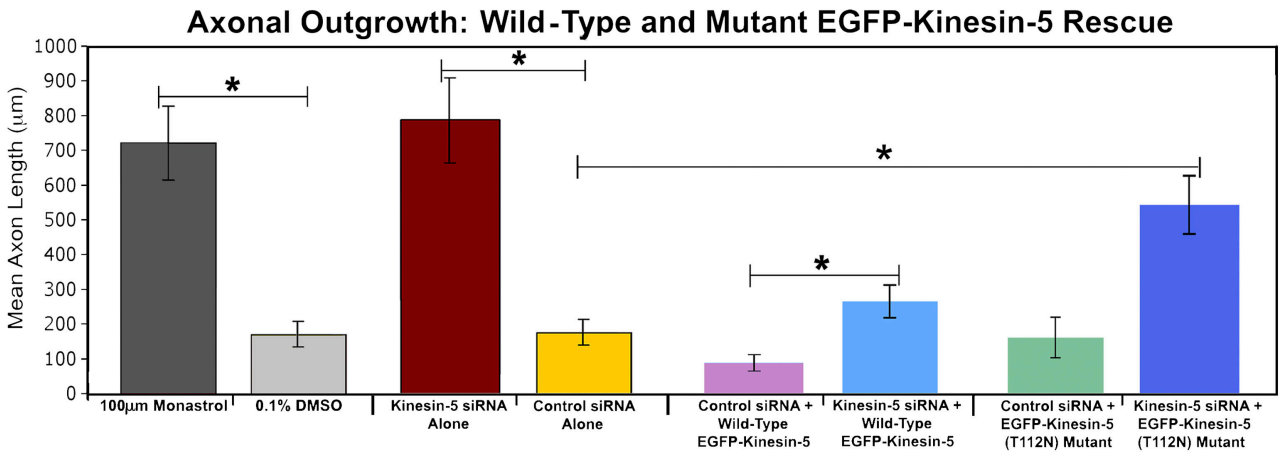


Figure 8. **Kinesin-5 elicits it effects in a force-dependent manner.** Inhibition of kinesin-5 by monastrol treatment or depletion of kinesin-5 by siRNA produces mean axonal lengths that are approximately four times greater than neurons treated with DMSO (control) or control siRNA. When a wild-type kinesin-5 construct is introduced into control siRNA–treated neurons, there is a corresponding diminution in mean axon length. Parallel experiments using a rigor mutant (T112N) kinesin-5 construct in control siRNA–treated neurons revealed that mean axonal lengths were indistinguishable from the control siRNA alone group. A similar effect was observed in kinesin-5–depleted neurons that were rescued by introduction of the wild-type EGFP–kinesin-5, with mean axonal lengths that were statistically similar to control siRNA neurons expressing endogenous levels of the motor protein (mean ± SEM, wild-type rescue = 257 ± 46.1 μm; control siRNA alone, 187 ± 37.1 μm; $P > 0.05$; two-tailed *t* test). Finally, in kinesin-5–depleted neurons that we attempted to rescue with the EGFP–kinesin-5 mutant, the mean length of axons were found to be nearly three times longer than the control siRNA–treated group, and more than twice the length of kinesin-5–depleted neurons rescued with wild-type kinesin-5 (mean ± SEM, rigor mutant rescue = 546 ± 86.5 μm; wild-type rescue, 257 ± 46.1 μm; $P < 0.002$; control siRNA alone, 187 ± 37.1 μm, $P < 0.001$; two-tailed *t* test). *, $P < 0.02$.

## Discussion

We previously speculated that kinesin-5 might be the motor that transports microtubules retrogradely in the axon, based on the premise that axonal growth rates may be determined by the ratio of anterograde/retrograde microtubule transport (Haque et al., 2004; Baas et al., 2006). In this view, depleting kinesin-5 would cause axons to grow faster because of a marked increase in this ratio. However, the current results show something quite different, i.e., that the frequency of microtubule transport in both directions is markedly increased when kinesin-5 is depleted. These results indicate that kinesin-5 is not the motor that transports microtubules retrogradely. Instead, it appears that kinesin-5 restricts the transport of short microtubules by other motors. The results of the depletion studies (Fig. 4) suggest that there is no directional preference on this effect, as removing kinesin-5 results in marked increases in both directions. In this sense, it may not be the ratio of anterograde/retrograde transport that is most critical to axonal growth, but rather, the overall vitality of the transport. The overexpression studies (Fig. 7), however, raise the possibility of a directional preference, suggesting that kinesin-5 may be more suited to opposing microtubule transport in the anterograde direction. This possibility is consistent with other studies in which kinesin-5 was shown to antagonize minus end–directed motors such as cytoplasmic dynein and kinesin-14a (Gaglio et al., 1996; Walczak et al., 1998; Mountain et al., 1999; Tao et al., 2006). It may be that kinesin-5 restricts microtubule transport in both directions, but preferentially in the anterograde direction.

Additional observations suggest that the greater length of kinesin-5–depleted axons is not solely explicable (or even principally explicable) on the basis of the changes in microtubule transport. The axons depleted of kinesin-5 are also far less prone to retraction, and this appears to be a major factor in their capacity to achieve greater lengths. This phenomenon is particularly evident with regard to the greater number of branches displayed by axons depleted of kinesin-5, where the numbers of branches appear to be dependent on the propensity of newly formed branches to retract. This is important because the proclivity of the axon to retract is not regulated by short microtubules, but rather by the microtubules that are long enough to act as compression-bearing struts (He et al., 2002; Baas et al., 2006; Myers et al., 2006b). Thus, we would contend that kinesin-5's principal role in regulating axonal length may be to influence the balance of forces on the long microtubules, which is consistent with our overall view that the various motors that transport microtubules are not selective for short microtubules but rather impinge upon microtubules of all lengths (Baas et al., 2006).

How does kinesin-5 elicits these effects? In the mitotic spindle, kinesin-5 is known to act between microtubules of opposite polarity orientation (interpolar microtubules). Although kinesin-5 was originally believed to function mainly to assist in the separation of the half spindles, newer studies indicate that it can alternatively function to resist separation of the half spindles by other motor proteins (Kapitein et al., 2005; Tao et al., 2006; Saunders et al., 2007). In this newer role, kinesin-5 has recently been likened to a brake on the microtubules within the spindle because it acts as a rate-limiting factor on the ability of the microtubules to slide relative to one another. The analogy of kinesin-5 acting as a brake on microtubule sliding is also quite applicable to our observations on the axon. The difference is that the mitotic spindle consists of regions of uniform and nonuniform microtubule polarity orientation, whereas nearly all of the microtubules in the axon are thought to be of the same orientation (Baas, 1998;

Hasaka et al., 2004). Thus it remains unclear whether the mechanism underlying the kinesin-5 brake is the same in the axon as in the mitotic spindle or one that is quite different.

It is important to note that kinesin-5 can also generate forces between neighboring microtubules of the same orientation within the mitotic spindle (Kapoor et al., 2000). Indeed, some of the earliest studies indicating antagonism between kinesin-5 and minus-end directed motors were conducted on monoasters of uniform polarity orientation (Gaglio et al., 1996). More recent studies suggest a complexity of possibilities for how kinesin-5 is able to generate different kinds of forces between microtubules of the same or different polarity orientations (Kapetein et al., 2005; Saunders et al., 2007). One possibility is that the two ends of the homotetramer are not always in synchrony with regard to force generation, thus generating options for the manner by which forces impact the relevant microtubules. It appears that kinesin-5 is also quite different from other kinesins with regard to how it reacts to changes in load (Valentine et al, 2006), which would likely influence kinesin-5's force-dependent functions. Whatever the case, understanding the complexities of force generation by kinesin-5 may clarify how kinesin-5 is capable of opposing transport of microtubules in both directions within the axon.

In discussing its mechanism of action, it is also important to consider that not all of the properties of kinesin-5 are force dependent. Kinesin-5 has been observed to cross-link neighboring microtubules (Sharp et al., 1999a) and to do so in a passive manner that does not require ATP (Tao et al., 2006). In this sense, kinesin-5 could antagonize microtubule sliding simply by cross-linking adjacent microtubules or by displacing other motors from the microtubule lattice, even when kinesin-5 is not undergoing a power stroke. Our studies using the rigor mutant indicate that the force-dependent properties of kinesin-5 are required for it to elicit its effects on axonal growth. Even so, we are reluctant to completely dismiss the possibility that the force-independent properties of kinesin-5 might contribute to its functions in the axon. For example, the growth cones of kinesin-5–depleted axons are clearly broader than those of control axons (Fig. 6), suggesting that the microtubules within these growth cones may be less cross-linked in the absence of kinesin-5. Thus it may be that the dual properties of kinesin-5 are manifested differently in the growth cone and in the axonal shaft. In this regard, it will be prudent in the future to conduct studies with the rigor mutant specifically on growth cone behaviors.

Another open question is whether kinesin-5 opposes all other motors equally, or if kinesin-5 specifically or preferentially antagonizes minus end–directed motors in the neuron. We have not yet studied kinesin-14a in neurons, but we have conducted a great deal of work on cytoplasmic dynein. As noted in the Introduction, these studies have enabled us to propose a model whereby cytoplasmic dynein generates forces between the longer microtubules in the axon and the cortical actin meshwork. These dynein-driven forces antagonize the contractile forces imposed on the cortical actin array by myosin-II (Ahmad et al., 2000; Myers et al., 2006b). Our finding that kinesin-5 promotes axonal retraction is consistent with a scenario by which forces generated by kinesin-5 antagonize the forces generated by cytoplasmic dynein. Our tentative thinking is that the microtubules nearest the cortex interact with the cortical actin via cytoplasmic dynein, and that these same microtubules sometimes interact with adjacent microtubules via kinesin-5. When the kinesin-5 is engaged there is an increase in the load on the cytoplasmic dynein, thereby attenuating its ability to antagonize the contractility of the cortical actin.

Clearly, an important goal for the future will be to further test the various possibilities of exactly how kinesin-5 elicits such a profound role in restricting the growth of the axon. In addition to elucidating its mechanism of action, an even more important question may be to ascertain why it is that developing neurons express such a potent brake on the growth potential of their axons. Also, of course, the question remains as to how kinesin-5's functions are regulated within the axon. In particular, local regulation of kinesin-5 would enable the axon to increase or decrease the relevant forces to comply with the needs of the axon. For example, branch formation would benefit both from a local increase in short microtubule transport and from a diminished propensity of the branch to retract once long microtubules have been established in the branch. This kind of regulation could be accomplished by signaling pathways, given that the association of kinesin-5 with microtubules is regulated by phosphorylation (Blangy et al., 1995; Sawin and Mitchison, 1995). Finally, it will be important to ascertain whether our findings on kinesin-5 apply to adult axons as well as developing axons because the ability to enhance axonal growth so dramatically by inhibiting kinesin-5 could be a powerful tool for augmenting axonal regeneration after injury (Baas, 2002).

## Materials and methods

**Cell culture and transfection**

Cultures of dissociated neurons from rat superior cervical ganglia were prepared as previously described (He et al., 2005). For experiments using siRNA, dissociated neurons were transfected with 10 μM (final concentration) of either control siRNA or kinesin-5 siRNA (*Silencer* KIF11 [Eg5] siRNA; Ambion). Once transfected, the neurons were cultured in L-15 medium on 35-mm plastic dishes that had been coated with 0.1 mg/ml poly-D-lysine (PDL) for 3 h and repeatedly rinsed in double-distilled $H_2O$. The following morning 5 μg/ml laminin and 5 μM arabinose C were added to the culture medium. For transport studies, the neurons were replated (He et al., 2005) at a density of ~7,500 cells/dish at 60 h after transfection onto grided glass coverslips that had been coated with 0.1 mg/ml PDL and 25 μg/ml laminin. Replating was performed 72 h after transfection. The EGFP-tubulin construct (CLONTECH Laboratories, Inc.) and the mCherry-tubulin construct (provided by R. Tsien, University of California, San Diego, La Jolla, CA) were transfected at 15 μg. Wild-type and mutant kinesin-5 constructs were provided by M. Kress (Institut André Lwoff, Centre National de la Recherche Scientifique, Villejuif, France) and A. Blangy (Centre de Recherches en Biochimie Macromoléculaire, Centre National de la Recherche Scientifique Unité Propre de Recherche, Montpellier, France), and then engineered in our laboratory as fusions with EGFP. The mutant construct, termed T112N, is described in detail by Blangy et al. (1998). For kinesin-5 overexpression studies, 12 μg of either GFP (control) or EGFP–kinesin-5 was cotransfected with mCherry-tubulin.

In one study, we wished to determine if expression of wild-type and/or the mutant kinesin-5 could "rescue" the phenotype obtained with siRNA-based depletion of kinesin-5. For these experiments, neurons were first transfected with siRNA. 48 h after transfection with siRNA, either the wild-type EGFP–kinesin-5 or the rigor mutant EGFP–kinesin-5 (T112N) was introduced using Lipofectamine 2000 (Invitrogen) as previously described (Yu et al., 2005), except that Lipofectamine treatments were performed for 4.5 h duration and were followed by rinsing and medium replacement with L-15 plating medium. Neurons were then replated 24–30 h after Lipofectamine

treatment and morphological analysis was performed as described below for siRNA experiments. Expression was observed in ~15–20% of neurons, and data analysis used neurons with expression levels greater than the mean expression value (determined by arbitrary fluorescence units) for that experimental group.

**Immunological techniques and Western blotting**
See the online supplemental Materials and methods.

**Morphological studies**
For all morphological investigations, neurons were cultured and replated after the 72-h replating regimen. For axonal length and branching experiments, neurons were identified at 1 h after replating (before they had established axons). The neurons were then imaged sequentially at 3, 5, and 7 h after replating. Axonal lengths were measured using the "measure/curve" application of Axiovision LE 4.5 (Carl Zeiss MicroImaging, Inc.), and mean values were quantified. Analysis of branching frequency was performed by counting the total number of branches per neuron and dividing these values by total axonal length for individual neurons. For both total branching and categorical branching analysis, we used normalization of branch number to total axonal length to ensure accurate evaluation of branching frequency.

**Nitric oxide–induced axonal retraction**
60 h after transfection with control or kinesin-5 siRNA, neurons were replated onto gridded PDL (0.1 mg/ml) and laminin-treated (25 μg/ml) glass-bottom culture dishes. By 72 h the neurons had generated extensive axons. The nitric oxide donor, noc-7 (Calbiochem), was prepared and applied as previously described (He et al., 2002), except that it was used at a working concentration of 0.3 mM. DIC images of axons were recorded before and 30 min after addition of noc-7. Axonal lengths (from growth cone to cell body or to the first bifurcation point) were measured using the "measure/curve" application in Axiovision LE 4.5. Raw data were processed and graphs were produced using Excel (Microsoft Corp.).

**Transport assays**
The microtubule transport assay was performed essentially as described previously (Hasaka et al., 2004), except that for experiments using pharmacological inhibition of kinesin-5 with monastrol, the neurons were plated directly onto glass coverslips in drug-containing medium and were imaged 24–36 h later. For siRNA-based studies, neurons transfected with either control siRNA or kinesin-5 siRNA were replated at 60 h as described in the previous paragraph. A total of 211 time-lapse images were taken at 700–900-ms exposure using 3-s intervals for each axon. Transport analysis included all microtubules observed to move continuously through the photobleached region during the imaging period. Transport frequencies were calculated by dividing the total number of movements by the total imaging time for individual movies.

**Vesicle and mitochondrion transport assays**
See the online supplemental Materials and methods.

**Live-cell imaging and analysis of stepwise axonal growth/retraction**
Neurons transfection with control or kinesin-5 siRNA (see Cell culture and transfection) were replated in L-15 medium (supplemented with FBS) onto PDL- and laminin (25 μg/ml)-coated glass coverslips. The L-15 medium was coated with 2 ml of mineral oil (Sigma-Aldrich) as a means to prevent medium evaporation and to maintain nutrient concentrations over time. Phase-contrast time-lapse images were acquired using either a 40 or 20× objective lens with 700-ms exposure time and 1 × 1 binning. Image acquisition was performed at 3-min intervals for 5 h using a heated stage apparatus to maintain the temperature at 37°C. Stepwise axon and branch growth were analyzed using the "Apps/Track Points" application of Metamorph software (Molecular Devices) by establishing a point of origin and then using automated tracking of axonal outgrowth. Data were exported from Metamorph to Excel and were analyzed for the relative change in distance to origin. A camera (Orca ER; Hamamatsu) was used. For additional details on statistical analysis and image processing, see online supplemental materials.

**Online supplemental material**
Video 1 shows that kinesin-5 depletion results in fewer bouts of retraction of axons and axonal branches. Online supplemental material is available at http://www.jcb.org/cgi/content/full/jcb.200702074/DC1.

We thank Gianluca Gallo and Jonathan Scholey for helpful discussions. We thank Anne Blangy and Michel Kress for providing kinesin-5 constructs and antibodies and Roger Y. Tsien for providing the mCherry-tubulin construct.

This work was supported by grants to P.W. Baas from the National Institutes of Health (NIH; R01NS28785), the Alzheimer's Association (IIRG-06-26604), the Department of the Army (GW060062), and the Craig H. Neilsen Foundation (2784). K.A. Myers was supported by a predoctoral National Research Service Award (SF3INS053022) from the NIH.

Submitted: 12 February 2007
Accepted: 9 August 2007

## References

Ahmad, F.J., J. Hughey, T. Wittmann, A. Hyman, M. Greaser, and P.W. Baas. 2000. Motor proteins regulate force interactions between microtubules and microfilaments in the axon. *Nat. Cell Biol.* 2:276–280.

Ahmad, F.J., Y. He, K.A. Myers, T.P. Hasaka, F. Francis, M.M. Black, and P.W. Baas. 2006. Effects of dynactin disruption and dynein depletion on axonal microtubules. *Traffic*. 7:524–537.

Baas, P.W. 1998. The role of motor proteins in establishing the microtubule arrays of axons and dendrites. *J. Chem. Neuroanat.* 14:175–180.

Baas, P.W. 2002. Microtubule transport in the axon. *Int. Rev. Cytol.* 212:41–62.

Baas, P.W., C. Vidya Nadar, and K.A. Myers. 2006. Axonal transport of microtubules: the long and short of it. *Traffic*. 7:490–498.

Blangy, A., H.A. Lane, P. d'Herin, M. Harper, M. Kress, and E.A. Nigg. 1995. Phosphorylation by p34cdc2 regulates spindle association of human Eg5, a kinesin-related motor essential for bipolar spindle formation in vivo. *Cell*. 83:1159–1169.

Blangy, A., P. Chaussepied, and E.A. Nigg. 1998. Rigor-type mutation in the kinesin-related protein HsEg5 changes its subcellular localization and induces microtubule bundling. *Cell Motil. Cytoskeleton*. 40:174–182.

Buckman, J.F., H. Hernandez, G.J. Kress, T.V. Votyakova, S. Pal, and I.J. Reynolds. 2001. MitoTracker labeling in primary neuronal and astrocytic cultures: influence of mitochondrial membrane potential and oxidants. *J. Neurosci. Methods*. 104:165–176.

Buster, D.W., D.H. Baird, W. Yu, J.M. Solowska, M. Chauviere, A. Mazurek, M. Kress, and P.W. Baas. 2003. Expression of the mitotic kinesin Kif15 in postmitotic neurons: implications for neuronal migration and development. *J. Neurocytol.* 32:79–96.

Crevel, I.M., M.C. Alonso, and R.A. Cross. 2004. Monastrol stabilises an attached low-friction mode of Eg5. *Curr. Biol.* 14:R411–R412.

Dent, E.W., J.L. Callaway, G. Szebenyi, P.W. Baas, and K. Kalil. 1999. Reorganization and movement of microtubules in axonal growth cones and developing interstitial branches. *J. Neurosci.* 19:8894–8908.

Ernst, A.F., G. Gallo, P.C. Letourneau, and S.C. McLoon. 2000. Stabilization of growing retinal axons by the combined signaling of nitric oxide and brain-derived neurotrophic factor. *J. Neurosci.* 20:1458–1469.

Ferhat, L., R. Kuriyama, G.E. Lyons, B. Micales, and P.W. Baas. 1998. Expression of the mitotic motor protein CHO1/MKLP1 in postmitotic neurons. *Eur. J. Neurosci.* 10:1383–1393.

Gaglio, T., A. Saredi, J.B. Bingham, M.J. Hasbani, S.R. Gill, T.A. Schroer, and D.A. Compton. 1996. Opposing motor activities are required for the organization of the mammalian mitotic spindle pole. *J. Cell Biol.* 135:399–414.

Haque, S.A., T.P. Hasaka, A.D. Brooks, P.V. Lobanov, and P.W. Baas. 2004. Monastrol, a prototype anti-cancer drug that inhibits a mitotic kinesin, induces rapid bursts of axonal outgrowth from cultured postmitotic neurons. *Cell Motil. Cytoskeleton*. 58:10–16.

Hasaka, T.P., K.A. Myers, and P.W. Baas. 2004. Role of actin filaments in the axonal transport of microtubules. *J. Neurosci.* 24:11291–11301.

He, Y., W. Yu, and P.W. Baas. 2002. Microtubule reconfiguration during axonal retraction induced by nitric oxide. *J. Neurosci.* 22:5982–5991.

He, Y., F. Francis, K.A. Myers, W. Yu, M.M. Black, and P.W. Baas. 2005. Role of cytoplasmic dynein in the axonal transport of microtubules and neurofilaments. *J. Cell Biol.* 168:697–703.

Kapitein, L.C., E.J. Peterman, B.H. Kwok, J.H. Kim, T.M. Kapoor, and C.F. Schmidt. 2005. The bipolar mitotic kinesin Eg5 moves on both microtubules that it crosslinks. *Nature*. 435:114–118.

Kapoor, T.M., T.U. Mayer, M.L. Coughlin, and T.J. Mitchison. 2000. Probing spindle assembly mechanisms with monastrol, a small molecule inhibitor of the mitotic kinesin, Eg5. *J. Cell Biol.* 150:975–988.

Kashina, A.S., R.J. Baskin, D.G. Cole, K.P. Wedaman, W.M. Saxton, and J.M. Scholey. 1996. A bipolar kinesin. *Nature*. 379:270–272.

Kwok, B.H., L.C. Kapitein, J.H. Kim, E.J. Peterman, C.F. Schmidt, and T.M. Kapoor. 2006. Allosteric inhibition of kinesin-5 modulates its processive directional motility. *Nat Chem Biol*. 2:480–485.

Lockhart, A., and R.A. Cross. 1996. Kinetics and motility of the Eg5 microtubule motor. *Biochemistry*. 35:2365–2373.

Ma, Y., D. Shakiryanova, I. Vardya, and S.V. Popov. 2004. Quantitative analysis of microtubule transport in growing nerve processes. *Curr. Biol.* 14:725–730.

Maliga, Z., and T.J. Mitchison. 2006. Small-molecule and mutational analysis of allosteric Eg5 inhibition by monastrol. *BMC Chem. Biol.* 6:2.

Maliga, Z., T.M. Kapoor, and T.J. Mitchison. 2002. Evidence that monastrol is an allosteric inhibitor of the mitotic kinesin Eg5. *Chem. Biol.* 9:989–996.

Mountain, V., C. Simerly, L. Howard, A. Ando, G. Schatten, and D.A. Compton. 1999. The kinesin-related protein, HSET, opposes the activity of Eg5 and cross-links microtubules in the mammalian mitotic spindle. *J. Cell Biol.* 147:351–366.

Myers, K.A., Y. He, T.P. Hasaka, and P.W. Baas. 2006a. Microtubule transport in the axon: re-thinking a potential role for the actin cytoskeleton. *Neuroscientist*. 12:107–118.

Myers, K.A., I. Tint, C.V. Nadar, Y. He, M.M. Black, and P.W. Baas. 2006b. Antagonistic forces generated by cytoplasmic dynein and myosin-II during growth cone turning and axonal retraction. *Traffic*. 7:1333–1351.

Pfister, K.K. 1999. Cytoplasmic dynein and microtubule transport in the axon: the action connection. *Mol. Neurobiol.* 20:81–91.

Saunders, A.M., J. Powers, S. Strome, and W.M. Saxton. 2007. Kinesin-5 acts as a brake in anaphase spindle elongation. *Curr. Biol.* 17:R453–R454.

Sawin, K.E., and T.J. Mitchison. 1995. Mutations in the kinesin-like protein Eg5 disrupting localization to the mitotic spindle. *Proc. Natl. Acad. Sci. USA*. 92:4289–4293.

Sharp, D.J., R. Kuriyama, R. Essner, and P.W. Baas. 1997. Expression of a minus-end-directed motor protein induces Sf9 cells to form axon-like processes with uniform microtubule polarity orientation. *J. Cell Sci.* 110:2373–2380.

Sharp, D.J., K.L. McDonald, H.M. Brown, H.J. Matthies, C. Walczak, R.D. Vale, T.J. Mitchison, and J.M. Scholey. 1999a. The bipolar kinesin, KLP61F, cross-links microtubules within interpolar microtubule bundles of *Drosophila* embryonic mitotic spindles. *J. Cell Biol.* 144:125–138.

Sharp, D.J., K.R. Yu, J.C. Sisson, W. Sullivan, and J.M. Scholey. 1999b. Antagonistic microtubule-sliding motors position mitotic centrosomes in *Drosophila* early embryos. *Nat. Cell Biol.* 1:51–54.

Tao, L., A. Mogilner, G. Civelekoglu-Scholey, R. Wollman, J. Evans, H. Stahlberg, and J.M. Scholey. 2006. A homotetrameric kinesin-5, KLP61F, bundles microtubules and antagonizes Ncd in motility assays. *Curr. Biol.* 16:2293–2302.

Walczak, C.E., I. Vernos, T.J. Mitchison, E. Karsenti, and R. Heald. 1998. A model for the proposed roles of different microtubule-based motor proteins in establishing spindle bipolarity. *Curr. Biol.* 8:903–913.

Wang, L., and A. Brown. 2002. Rapid movement of microtubules in axons. *Curr. Biol.* 12:1496–1501.

Weil, D., L. Garcon, M. Harper, D. Dumenil, F. Dautry, and M. Kress. 2002. Targeting the kinesin Eg5 to monitor siRNA transfection in mammalian cells. *Biotechniques*. 33:1244–1248.

Yoon, S.Y., J.E. Choi, J.W. Huh, O. Hwang, H.S. Lee, H.N. Hong, and D. Kim. 2005. Monastrol, a selective inhibitor of the mitotic kinesin Eg5, induces a distinctive growth profile of dendrites and axons in primary cortical neuron cultures. *Cell Motil. Cytoskeleton*. 60:181–190.

Yu, W., and P.W. Baas. 1994. Changes in microtubule number and length during axon differentiation. *J. Neurosci.* 14:2818–2829.

Yu, W., J.M. Solowska, L. Qiang, A. Karabay, D. Baird, and P.W. Baas. 2005. Regulation of microtubule severing by katanin subunits during neuronal development. *J. Neurosci.* 25:5573–5583.